The Recent Increase in North Atlantic Wave Heights*

Y. KUSHNIR

Lamont-Doherty Earth Observatory, Palisades, New York

V. J. CARDONE AND J. G. GREENWOOD

Oceanweather Inc., Cos Cob, Connecticut

M. A. CANE

Lamont-Doherty Earth Observatory, Palisades, New York

(Manuscript received 6 March 1996, in final form 5 December 1997)

ABSTRACT

The nature and causes of the recent increase in North Atlantic wave heights are explored by combining a numerical hindcast with a statistical analysis. The numerical hindcast incorporates a 10-yr history (1980–89) of North Atlantic, twice daily wind analyses to generate a monthly averaged significant wave height (SWH) history. The hindcast compares favorably with published monthly averaged SWH observations. The link between model-generated wintertime monthly SWH and monthly averaged sea level pressure (SLP) data is determined by means of a canonical correlation analysis (CCA). Within the analysis domain, most of the variance in SWH and SLP is captured by two pairs of joint patterns. The leading pair consists of a SLP dipole resembling the North Atlantic Oscillation (NAO) and a SWH dipole in spatial quadrature relation to it. Using the CCA results, an extended statistical hindcast of monthly wave fields is generated from sea level pressure data and used to quantitatively estimate the systematic increase in wave heights since the 1960s. It is shown that an increasing trend in SWH at several northeast Atlantic locations since 1960 or so is related to the systematic deepening of the Icelandic low and intensification of the Azores high over the last three decades. The analysis suggests that wave height south of 40°N has decreased during the same period.

1. Introduction

In the discussion of climate change and variability, the effect of large-scale circulation changes on the intensity, frequency, and location of individual storms is of great concern (e.g., Houghton et al. 1990). Over the oceans, the cumulative effect of changes in storminess is manifested in surface wave-climate variability, with consequences to the operation and safety of shipping, offshore industries, and coastal development. Concerns about changes in ocean wave climate have heightened in recent years due to increasing reports of extreme wave heights encountered in individual severe storms. These reports could be due to recent improvements in the observational networks (automated deep water buoys), or to an increase is merchant ships' ability to withstand rough seas, and thus report on higher waves. However, it is quite likely that these reports are due to systematic intensification of severe storms over time, or to their increased frequency of occurrence, as part of a long-term climatic trend or oscillation.

In their study of North Atlantic wave climate variability, Bacon and Carter (1991, hereafter referred to as BC91) tabulated reliable instrumental observations of monthly mean significant wave height (SWH) at two locations: the Ocean Weather Ship (OWS) Lima (57°N, 20°W) from 1975 to 1988; and the *Seven Stones* Light Vessel (SSLV, off Lands End in southwestern England), from 1962 to 1986. These records are consistent and long enough to demonstrate the existence of a systematic increase in annual-mean SWH from the 1960s to the 1980s in the eastern North Atlantic (BC91). In a subsequent study, Bacon and Carter (1993, hereafter BC93) compared the trend in wave heights with the trend in the north–south sea level pressure (SLP) gradient across the basin (between the Azores and Iceland) and concluded that the two are linked. These results indicate an

* Lamont-Doherty Earth Observatory Contribution Number 5644.

Corresponding author address: Yochanan Kushnir, Lamont-Doherty Earth Observatory, Columbia University, Route 9W, Palisades, NY 10964.

increase in storminess in the North Atlantic region and point at large-scale circulation changes as the culprit.

In the present study, we seek to establish, in a systematic and quantitative manner, the relationship between North Atlantic wave climate variability and the low-frequency variability of the atmospheric circulation. Furthermore, we would like to exploit this relationship to strengthen the hypothesis (e.g., BC91 and BC93) that the trend in North Atlantic storminess is real and stems from systematic changes in meteorological conditions. Given the quality of numerical wave prediction models, it seems that the preferred way for achieving the goal of generating an extended and accurate time-dependent depiction of the surface wave field is to numerically hindcast the latter from historical surface meteorological data (winds). Such hindcast attempts have proved quite successful in several case studies (e.g., Cardone et al. 1996), and efforts to apply them to create longer wave height records for climatological applications are under way (WASA 1995). However, the task is far from simple, as historical surface wind data, from weather buoys and merchant ship observations, are nonuniformly distributed in space and time, and subject to systematic errors (Cardone et al. 1990; Ward and Hoskins 1996). A careful analysis of available wind data such as used in case studies is a time consuming operation (Cardone et al. 1996), and attempts to create an extended and temporally consistent numerical assimilation of meteorological data have just begun (e.g., Kalnay et al. 1996).

In this study we offer an alternative way to capture the basic features of the surface wave field long-term variability, while work to establish a temporally and spatially more detailed wave hindcast is continued. We use, as discussed in section 2, a relatively short and reasonably consistent record (10 yr) of twice-daily surface wind analyses, to create a comparable record of SWH hindcast fields. The link between monthly mean SWH and SLP is subsequently determined using data from this numerical hindcast. We show (in section 3b) that on a monthly timescale a strong, linear relationship exists between these fields. Since SLP observations are robust, and their long time history is relatively free from systematic instrumental errors, we are able to depict from the statistical SWH–SLP relationship, the long-term temporal evolution of the surface wave field, and show in section 3c, that the trend in hindcast SWH is consistent with observations.

2. Numerical wave hindcast procedure

On a day-to-day basis, ocean surface waves are determined by the recent history of local and remote surface winds (e.g., Kinsman 1965). The complex, nonlocal relationship between the surface wind field and the wave spectrum is captured by modern numerical wave models (Komen et al. 1994). Cardone et al. (1996) show that given high quality wind data, such models are capable of simulating, to a high level of accuracy, the observed properties of the wave field.

In the present study, we obtain forcing data for the numerical hindcast from the operational 1000-hPa-level wind analysis of the European Centre for Medium-Range Weather Forecasts (ECMWF, e.g., Trenberth et al. 1990[1]). The data available for this study cover the period from 1 January 1980 to 31 December 1989, at 12-h intervals. The zonal and meridional wind components are given on a global 2.5° lat × 2.5° long grid from which the North Atlantic sector (equator to 70°N) was extracted. It was not expected that these wind data, which are of lesser quality than the winds used in specific case studies such as indicated above, will yield the same high quality day-by-day wave simulation. We nonetheless anticipated that these wind data will produce a reliable simulation of the SWH field when monthly averaged data are concerned. Of course the 1000-hPa level is strictly not equivalent to some fixed height above the sea level, as required by the ocean model. However, in practice, assimilation of surface marine data in the ECMWF analysis system, used through at least 1986, assigned the measured winds to the 1000-hPa level (Trenberth et al. 1990), making this level the effective surface marine wind level.

The exact analysis height of the analyzed winds cannot be specified because the observations are generally not adjusted to a standard height before the assimilation. A simple adjustment of the analyzed wind speed was therefore performed to provide winds approximately representative of the 20-m level, as required by the present wave model. The adjustment was achieved by comparing ECMWF winds to synoptic wind observations at OWS Lima (57°N, 20°W) and Mike (66°N, 3°E), for all available reports from 1983 to 1989. Systematic differences between analysis and observations were expressed as the mean ratio of 1000-hPa wind speed to OWS wind speed, and mean difference of 1000-hPa wind direction to OWS wind direction, in regular bins of 1000-hPa speed and direction. Without other overlapping, high quality observations, these binned differences were applied to adjust the 12-h 1000-hPa winds at all grid points in the North Atlantic from the equator to 70°N. This correction is no doubt rudimentary, and its success was judged a posteriori by comparing observed wave statistics to the hindcast values (see below). It should also be noted that we did not detect any discontinuity in the ECMWF 1000-hPa analysis despite several changes in assimilation procedure during the time interval 1980–89.

[1] Data available through the National Center for Atmospheric Research (NCAR), Boulder, Colorado.

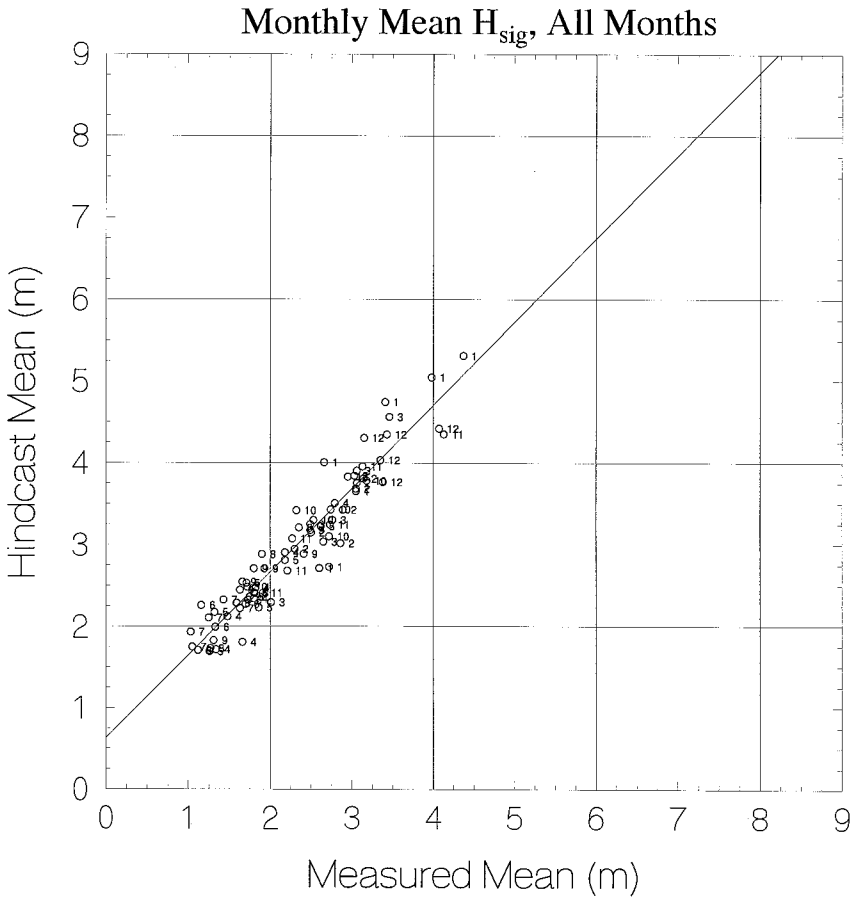

FIG. 1. Scatterplot of monthly averaged hindcast significant wave height at a grid point closest to SSLV vs observations there. Units are in m.

The adjusted ECMWF winds were used to force a well-tested, ''first generation'' discrete spectral wave model, with demonstrated skill in the specification of integrated properties of the wave spectrum, such as the SWH (Khandekar et al. 1994). The resulting 10-yr hindcast was found to reproduce the observed monthly mean conditions at SSLV and Lima, with an overall correlation of 0.95, and 0.91, respectively. The scatterplot of observed waves at SSLV vs the hindcast at the closest model grid point is shown in Fig. 1. The figure depicts a good relationship, at all heights. The results do exhibit a small bias, independent of the wave height, such that hindcast SWH is somewhat higher than the observed.

3. Statistical extension of numerical hindcast

a. Canonical correlation analysis of numerical hindcast SWH fields and corresponding SLP data

To examine the long-term climatic variability of North Atlantic waves, we needed to extend the wave hindcast to years that predate the ECMWF analysis. For this purpose we sought to construct a statistical model that links monthly mean SWH fields to some large-scale indicator of monthly mean meteorological conditions. As indicated above, the surface wind field is the marine meteorological variable most directly linked to wave heights, but its long-term record displays systematic errors due to changes in observational practices. However, the SLP record (dynamically linked to the wind by a nearly diagnostic relationship) has been considered free of such systematic errors (e.g., Ward and Hoskins 1996), and is, therefore, the preferred variable for establishing the long-term evolution of the wave field through statistical methods.

The first step in the statistical extension of the numerical hindcast was to establish the relationship between monthly mean ECMWF SLP analyses, and the simultaneous hindcast SWH fields. Monthly mean SLP fields were calculated from the ECMWF 1000-hPa height field. Anomalies from the mean annual cycle of SLP and SWH field were then subjected to a canonical correlation analysis (CCA). This analysis is described by Barnett and Preisendorfer (1987, see also Bretherton et al. 1992; Zor-

ita et al. 1992). The procedure finds the leading principal components (PCs) of each dataset separately and then calculates the linear combination of these PCs that maximizes the temporal correlation between the two variables. Since the observed trend in SSLV is most prominent in the cold-season months (November to March), only data for these months were considered.

In the present analysis, four leading PCs of SLP and two of SWH were used. These account for 75% and 64% of the SLP and SWH variance, respectively. The number of PCs was decided based on the North et al. (1982) criterion for determining error in eigenvalues, and Preisendorfer's rule N (Preisendorfer 1988) that compares the actual eigenvalue distribution with a null hypothesis assuming no large-scale signal in the data. The CCA yields two joint "modes" of SLP and SWH variability.

b. Observed link between monthly SWH and SLP anomalies

Before we continue to describe the statistical extension of the numerical hindcast, we examine the statistical relationship between the SLP and SWH fields as revealed in the CCA. The spatial patterns of the two joint canonical modes of SLP and SWH are shown in Fig. 2. The first pattern of SLP (Fig. 2a) indicates a perturbation resembling the much studied North Atlantic Oscillation (NAO), a seesaw in pressure variations between Iceland and the Azores (e.g., van Loon and Rogers 1978; Lamb and Peppler 1987). The associated SWH pattern has centers of action west of the British Isles and in the middle of the subtropical North Atlantic. The analysis implies that when SLP is higher (lower) than normal near Iceland and lower (higher) than normal near the Azores, waves are lower (higher) than normal in the northeast Atlantic, and higher (lower) than normal along 30°N. The second CCA pattern (Fig. 2b) describes a link between wave heights in the southeastern North Atlantic and a modulation of the westerlies there by an SLP perturbation resembling the eastern Atlantic teleconnection pattern (Wallace and Gutzler 1981). These modes of SLP–SWH association can be understood in the context of the related large-scale changes in wind circulation over the analysis domain.

The two described pairs of canonical correlation patterns capture 38% and 12% of the area-integrated SLP variance, and 37% and 27% of the area-integrated SWH variance. Compared to the 1980–89 numerical wave hindcast results, the first and second CCA patterns explain 60% and 10% of the SWH variance, respectively, at a grid point closest to SSLV. The corresponding numbers at a grid point closest to Lima are 86% and 1%, respectively. The CCA time series corresponding to SLP and SWH correlate highly with one another. The correlation is 0.97 for the time series corresponding to the first canonical pair and 0.83 for the second pair. The high correlation values indicate a strong and coherent linear relationship.

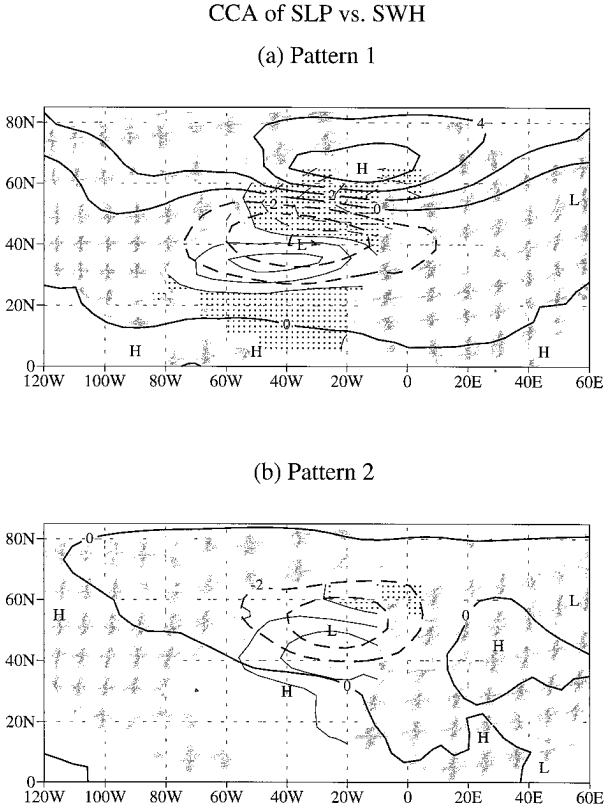

FIG. 2. Canonical patterns of the cold season (November–March) sea level pressure (SLP) and significant wave height (SWH) in the North Atlantic sector, 1980–1989. SLP is depicted by the heavy contours every 2 hPa, negative contours are dashed. SWH is depicted by thin contours every 0.2 m, negative areas are stippled. (a) The leading canonical pair, and (b) the second pair.

The results of the CCA can be used to determine the state of one multivariate dataset given the time history of the other, in a procedure akin to multiple regression (Graham and Michaelsen 1987; Barnston and Ropelewski 1992). Monthly mean ECMWF SLP data were used to determine the monthly mean SWH. As demonstrated in Fig. 3, the CCA based prediction captures between 50% and 90% of the variance in the numerical hindcast, north of 30°N, depending on the geographical location.

c. Historical SWH variations from statistical hindcast

As the final step in the statistical extension of the numerical hindcast to years preceding the ECMWF analysis, we used historical SLP data from COADS (Comprehensive Ocean Atmosphere Data Set, Woodruff

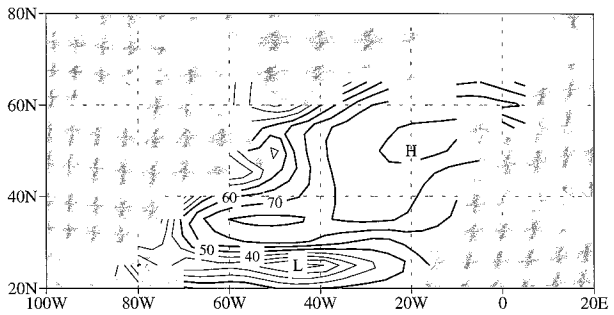

FIG. 3. The correlation (×100) between the numerical hindcast monthly mean SWH and the canonical correlation analysis projection from sea level pressure data. Correlation is calculated at each grid point using data for the cold season from 1980 to 1989.

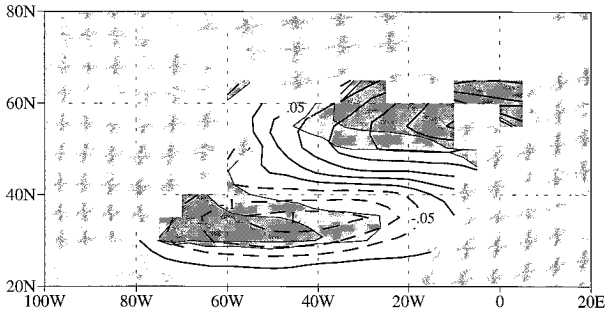

FIG. 4. The basinwide trend in cold-season significant wave height, from 1962 to 1986, as determined from the present statistical–numerical hindcast. Contours are in intervals of 0.05 m per decade. Areas with high statistical significance are shaded, with light and dark shading implying significance at the 90%–95% level and >95% level, respectively.

et al. 1987[2]) to determine the temporal evolution of the two SLP patterns. The standardized SLP difference between 65°N, 15°W and 40°N, 35°W (the two centers of action of the first CCA pattern) was used as an index for the time evolution of the first pattern. Similarly, the standardized SLP near 50°N, 30°W served as an index for the second pattern. With such simply constructed indices it is possible to trace the history of the patterns back to the 1920s. Here however, we focus on the last few decades only.

The SWH values determined from our statistical procedure agree reasonably well with the monthly mean wave height data at SSLV and Lima as tabulated in BC91 (correlation of 0.72 and 0.61, respectively). Moreover, the North Atlantic SWH determined in the statistical procedure displays significant trend during the interval 1962–86 as shown in Fig. 4. Clearly, our numerical–statistical hindcast confirms the increase in cold-season, northeast Atlantic wave heights at a rate of up to 0.3 m decade^{-1}. The analysis also suggests that south of 40°N wave heights decreased by a rate of up to 0.2 m decade^{-1}. At SSLV our analysis yields a positive trend in cold season SWH of 0.19 m decade^{-1} (0.21 m decade^{-1} if only months with SSLV observations are used) compared to a trend of 0.26 m decade^{-1} in the observations (Fig. 5). These trends, derived from the least squares linear fits to the data, are different from zero at the 99% level and their 95% confidence interval is approximately 0.15 m per decade.

[2] Data offered in netCDF format by the Climate Diagnostics Center, ERL/NOAA. Boulder, Colorado.

4. Conclusions

Examination of the 1950–1992 SLP time series corresponding to the first CCA pattern (Fig. 6) reveals the origin of the trend in wave heights. The pressure difference between Iceland and the Azores displays a negative trend with time, in particular after 1960. This corresponds to the concurrent positive trend in the strength of the seasonally averaged westerlies north of 40°N. The

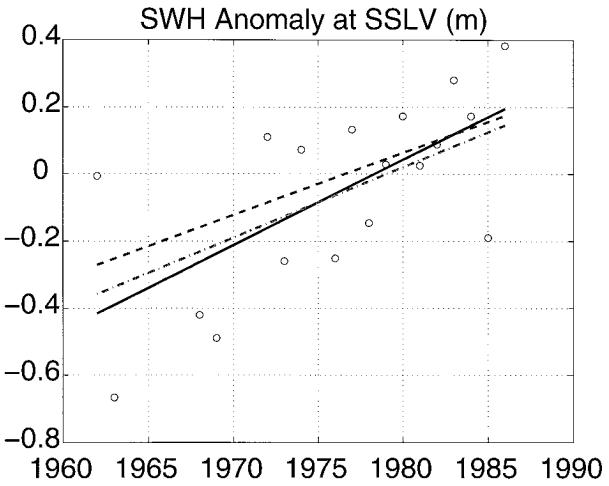

FIG. 5. The least squares linear trend fitted to cold-season (November–March) average SSLV observations (solid line) and the trend according to the statistical–dynamical hindcast at the closest grid point (dashed line). The dotted–dashed line is the trend fitted to hindcast data taken only for seasons with available SSLV observations. Also shown are the observed cold-season-averaged significant wave height anomalies at SSLV (circles). Abscissa is SWH anomaly in m.

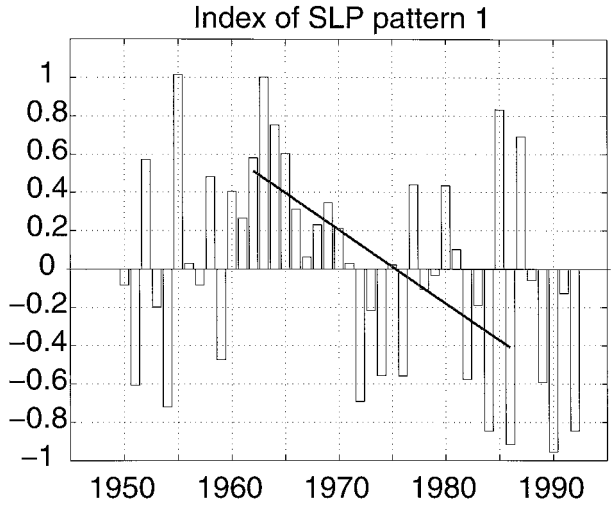

FIG. 6. Time series of cold-season-average normalized sea level pressure difference between 65°N, 15°W and 40°N, 35°W from 1950 to 1992. Also shown is the trend line fitted to cold-season averages from 1962 to 1986. The trend in the normalized SLP index is −0.38 per decade corresponding to a 2.46 hPa per decade in the pressure increase gradient between Iceland and the Azores from 1962 to 1986. Abscissa is the standardized pressure difference between the grid points corresponding to the maximum and minimum pressure in Fig. 1a.

long-term SLP trend was previously noted by BC93 and discussed in a broader context by Kushnir (1994) and Hurrell (1995). The cause of the trend in the seasonal SLP distribution is unknown. While it might present a unique change in the climate system, longer time series (Kushnir 1994; Hurrell 1995) and proxy data (D'Arrigo et al. 1993) suggest there have been slow up- and downswings in basin SLP in the past. Thus, the present trend may prove to be part of a natural fluctuation.

The present study adds quantitative support to the reported increase in North Atlantic SWH and uses a physical model of ocean surface wave equations to clearly demonstrate that the trend in surface meteorological conditions is the cause for this increase. The use of a multivariate analysis lends more credibility to the observations and the previous analyses (BC91 and BC93).

The degree of linear association between the monthly averaged SLP and the SWH fields, revealed in the present analysis, is striking and perhaps surprising because the actual day-to-day variability of SWH is determined by a complex, nonlinear, and nonlocal interaction. However, the large-scale monthly mean SLP field is closely related to the strength and to the spatial and temporal distribution of synoptic-scale weather perturbations. This relationship, revealed in previous studies (e.g., Lau 1988; Rogers 1990), may explain the strong linear association between SLP and SWH.

As mentioned earlier (section 2), efforts are under way to construct a high-resolution and more detailed depiction of North Atlantic wave climate variability. These efforts are no doubt important to determine additional information beyond the rudimentary aspect of the present analysis. Such analysis will account for the missing part of the wave variance not captured in the present study (see Fig. 2 above). It will also provide complete information on the wave spectrum that is crucial to application such as marine and coastal engineering.

Acknowledgments. This study was made possible by Grant NA56GP0161 from the NOAA Office of Global Programs and Grant JPLCIT957647 from the NASA Jet Propulsion Laboratory. We thank three anonymous reviewers for useful comments that helped improve this manuscript.

REFERENCES

Bacon, S., and D. J. Carter, 1991: Wave climate changes in the North Atlantic and North Sea. *Int. J. Climatol.,* **11,** 545–558.

——, and J. T. Carter, 1993: A connection between mean wave height and atmospheric pressure gradient in the North Atlantic. *Int. J. Climatol.,* **13,** 423–436.

Barnett, T. P., and R. W. Preisendorfer, 1987: Origin and levels of monthly and seasonal forecast skill for United States surface air temperatures determined by canonical correlation analysis. *Mon. Wea. Rev.,* **115,** 1825–1850.

Barnston, A. G., and C. F. Ropelewski, 1992: Prediction of ENSO episodes using canonical correlation analysis. *J. Climate,* **5,** 1316–1345.

Bretherton, C. S., C. Smith, and J. M. Wallace, 1992: An intercomparison of methods for finding coupled patterns in climate data. *J. Climate,* **5,** 541–560.

Cardone, V. J., J. G. Greenwood, and M. A. Cane, 1990: On trends in historical marine data. *J. Climate,* **3,** 113–127.

——, R. E. Jensen, D. T. Resio, V. R. Swail, and A. T. Cox, 1996: Evaluation of contemporary oceanwave models in rare extreme events: ''Halloween storm'' of October 1991 and the ''storm of the century'' of March 1993. *J. Atmos. Oceanic Technol.,* **13,** 198–230.

D'Arrigo, R. D., E. R. Cook, G. C. Jacoby, and K. R. Briffa, 1993: NAO and sea surface temperature signatures in tree-ring records from the North Atlantic Sector. *Quat. Sci. Rev.,* **12,** 431–440.

Graham, N. E., and J. Michaelsen, 1987: An investigation of the El Niño–Southern Oscillation cycle with statistical models. 2. Model results. *J. Geophys. Res.,* **92,** 14 271–14 289.

Houghton, J. T., G. J. Jenkins, and J. J. Ephramus, Eds., 1990: *Climate Change. The IPCC Scientific Assessment.* Cambridge University Press, 365 pp.

Hurrell, J. W., 1995: Decadal trends in the North Atlantic Oscillation: Regional temperatures and precipitation. *Science,* **269,** 676–679.

Kalnay, E., and Coauthors, 1996: The NCEP/NCAR 40-year reanalysis project. *Bull. Amer. Meteor. Soc.,* **77,** 437–471.

Khandekar, M. L., R. Lalbeharry, and V. J. Cardone, 1994: The performance of the Canadian ocean wave model (CSOWM) during the Grand Banks ERS-1 SAR Wave Spectra Validation Experiment. *Atmos.–Ocean,* **32,** 31–60.

Kinsman, B., 1965: *Wind Waves, Their Generation and Propagation on the Ocean Surface.* Prentice-Hall, 676 pp.

Komen, G. J., L. Cavalieri, M. Donelan, K. Hasselmann, S. Hasselmann, and P. A. E. M. Janssen, 1994: *Dynamics and Modeling of Ocean Waves.* Cambridge University Press, 532 pp.

Kushnir, Y., 1994: Interdecadal variations in North Atlantic sea surface temperature and associated atmospheric conditions. *J. Climate,* **7,** 141–157.

Lamb, P. J., and R. A. Peppler, 1987: North Atlantic oscillation:

Concept and an application. *Bull. Amer. Meteor. Soc.,* **68,** 1218–1225.

Lau, N. C., 1988: Variability of observed midlatitude storm tracks in relation to low-frequency changes in the circulation pattern. *J. Atmos.. Sci.,* **45,** 2718–2743.

North, G. R., T. L. Bell, R. F. Cahalan, and F. J. Moeng, 1982: Sampling errors in the estimation of empirical orthogonal functions. *Mon. Wea. Rev,* **110,** 699–706.

Preisendorfer, R. W., 1988: *Principal Component Analysis in Meteorology.* Development in Atmospheric Sciences, Vol. 17, Elsevier, 425 pp.

Rogers, J. C., 1990: Patterns of low-frequency monthly sea level pressure variability (1899–1986) and associated wave cyclone frequencies. *J. Climate,* **3,** 1364–1379.

Trenberth, K. E., W. G. Large, and J. G. Olson, 1990: The mean annual cycle in global wind stress. *J. Phys. Oceanogr.,* **20,** 1742–1760.

van Loon, H., and J. C. Rogers, 1978: The seesaw in winter temperatures between Greenland and northern Europe. Part I: General description. *Mon. Wea. Rev.,* **106,** 296–310.

Wallace, J. M., and D. S. Gutzler, 1981: Teleconnections in the geopotential height field during the Northern Hemisphere winter. *Mon. Wea. Rev.,* **109,** 784–812.

Ward, M. N., and B. J. Hoskins, 1996: Near-surface wind over the global ocean 1949–1988. *J. Climate,* **9,** 1877–1895.

WASA, 1995: The WASA project: Changing storm and wave climate in the North Atlantic and adjacent seas? *Fourth Int. Workshop on Wave Hindcasting and Forecasting,* Banff, AB, Canada, Panel on Energy Research and Development, 31–34.

Woodruff, S. D., R. J. Slutz, R. L. Jenne, and P. M. Steurer, 1987: A Comprehensive Ocean–Atmosphere Data Set. *Bull. Amer. Meteor. Soc.,* **68,** 1239–1250.

Zorita, E., V. Kharin, and H. von Storch, 1992: The atmospheric circulation and sea surface temperature in the North Atlantic area in winter: Their interaction and relevance for Iberian precipitation. *J. Climate,* **5,** 1097–1108.